Modeling of continuous steel coating by self-induced ion plating (SIP)

Antonella Contino[1], Véronique Feldheim[1], Paul Lybaert[1], Benoît Deweer [2]
[1]Faculté Polytechnique de Mons - Service de Thermique et Combustion
Rue de l'Epargne, 56 – 7000 Mons - Belgium
E-Mail: Antonella.Contino@fpms.ac.be, Veronique.Feldheim@fpms.ac.be, Paul.Lybaert@fpms.ac.be
[2] RDCS – Groupe Arcelor, Liège, Belgium
E-Mail: Benoit.Deweer@cockerill-sambre.com

Abstract

The present communication deals with the study of a new physical vapor deposition process called self-induced ion plating (SIP). This process is developed to produce continuous coating of flat products in the steel industry. The aim of this paper is to present a numerical simulation model of the SIP process. The aim of this model is to predict the thickness profile of the coating deposited on the substrate. The simulation of the SIP process is based on three coupled models. The first one deals with magnetism and simulates a magnetron system, the second one defines the heat transfer phenomena that occur in the SIP process and the last one determines the thickness profile of the coating on the substrate using the theory of evaporation. The computed thickness profile is then compared to the measured one.

I. Introduction

The self-induced ion plating (SIP) [1] is a new physical vapor deposition process developed in order to produce continuous coating of flat products in the steel industry. This technique is based on two well-known PVD processes: the vacuum evaporation and the magnetron sputtering. The SIP presents the advantages of both techniques: the high deposition rate of the vacuum evaporation and the good adherence of the deposit layer generated by a magnetron sputtering process.

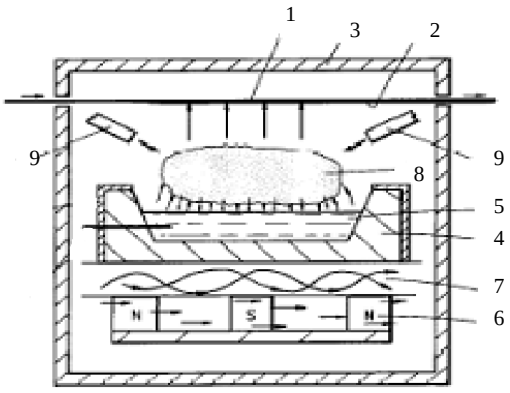

1. Substrate
2. Deposit layer
3. Enclosure
4. Crucible
5. Target
6. Permanent magnets (Magnétron)
7. Thermal resistance
8. Plasma
9. Gas injectors

Figure 1. SIP process [2]

The SIP process (figure 1) operates under high vacuum ($\cong 10^{-3}$-10^{-4} Torr). Argon gas is ionized between the cathode (target of tin, zinc, …) and the anode (substrate of steel) to produce plasma. The argon ions (Ar^{+}), created by the collisions that occur between electrons and argon atoms, are accelerated in the sheath of the plasma towards the target contained in a refractory crucible. The bombardment of those ions heats the liquid target and leads to its evaporation. To prevent the cooling of the crucible a layer of insulating powder is placed under it.

Another consequence of the bombardment is the electrons extraction out of the target. Those electrons, called secondary electrons, are accelerated in the sheath of the plasma towards the bulk of the plasma and gain enough energy to ionize argon atoms. They are then useful to maintain the plasma.

The plasma created in the process is confined near the target by a magnetic field. This confinement has as consequence a power distribution that presents a maximum where the magnetic field lines are parallel to the cathode. This non-uniform distribution is revealed in experiments by the presence of an erosion track at the target surface (figure 2).

Figure 2. Track of erosion

This magnetic field is generated by permanent magnets (magnetron) disposed under the target. This confinement increases the ions bombardment of the cathode and the throughput of the process. So, very high deposition rates can be achieved with moderate values of the electrical mean power density applied to the target. The magnets are cooled by a water flow to maintain their high residual magnetism (≅ 1 Tesla) .

The aim of the present work is to develop a numerical simulation model of the SIP process in order to predict the thickness profile of the coating deposited on the substrate. The simulations are carried out with the interactive environment MATLAB® and FEMLAB®, a tool for PDE-based multiphysics modeling in MATLAB®.

The simulation of the SIP process is based on three coupled models. The first one deals with magnetism. We evaluate the magnetic field generated by the magnetron in order to define the power distribution applied by the ions bombardement to the target surface. The second one deals with the heat transfer phenomena i.e. thermal conductivity and radiation (possible convective phenomena inside the crucible are neglected in this first approach) that occur between all the components of the SIP process. The last model determines the thickness profile of the coating on the substrate using the temperature field obtained in the previous step and the theory of evaporation.

II. Magnetic model

The first step in the simulation of the SIP process is the evaluation of the magnetic field created by the magnetron and surrounding the target. In fact, we will use this information to define the power distribution imposed on the target surface.

In a current free region $\vec{\nabla}\times\vec{H}=0$, we can define the scalar magnetic potential V_m as $\vec{H}=-\vec{\nabla}V_m$.
The relationship between the magnetic flux density $\vec{B}$ and the magnetic field $\vec{H}$ is given by

$$\vec{B}=\mu_0(\vec{H}+\vec{M}) \qquad (1)$$

where $\vec{M}$ (A m^{-1}) is the magnetization and μ_0 ($4\pi 10^{-7}$ H m^{-1}) is the vacuum permeability.

Using a linear expression for the magnetization,

$$\vec{M}=\vec{M}_0+(\mu_r-1)\vec{H} \quad (2)$$

where $\vec{M}_0$ (Am^{-1}) is the pre-magnetization of the magnets and μ_r, the relative permeability of the material, we obtain the relation

$$\vec{B}=\mu_0\mu_r\vec{H}+\mu_0\vec{M}_0 \quad (3)$$

Considering also $\vec{\nabla}\vec{B}=0$, we can determine V_m with the following equation :

$$-\vec{\nabla}(\mu_0\mu_r\vec{\nabla}V_m-\mu_0\vec{M}_0)=0 \quad (4)$$

As boundary condition we impose, far enough from the magnets, the following condition :

$$\vec{n}\vec{B}=0\rightarrow\vec{n}(\mu_0\mu_r\vec{\nabla}V_m-\mu_0\vec{M}_0)=0 \quad (5)$$

The differential equation (4) is solved with FEMLAB®.

The results, obtained for a quarter of the SIP geometry, are presented below. On figure 3 we can compare computed vertical magnetic induction at the target level with measurements. Taking into account that the maximum value of the magnetic induction component is simulated with an approximate error of 10 % compared to the measured one, we notice an excellent agreement between the measurements and the results of the FEMLAB® model .

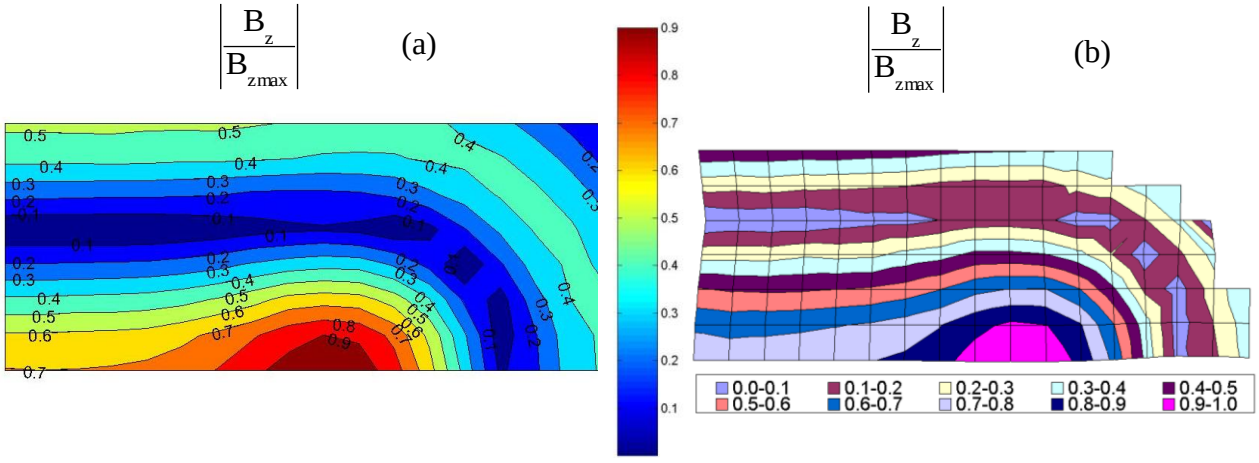

Figure 3. Simulated (a) and measured (b) vertical component of magnetic induction (normalized field with the maximum value of the component).

Experiments [3] show that the depth of erosion depends upon the angle at which ions hit the target. If we define θ, the angle between the incident ion direction and the normal to the target surface, as :

$$\cos(\theta)=\frac{B_{xy}}{\sqrt{B^2_{xy}+B^2_z}} \quad (6)$$

it is noted that a graph of $cos^3\,\theta$ is remarkably close to the erosion profile.

In this paper, we suppose that the ion bombardement heat flux evolves as the erosion profile. In fact, if the magnetic field lines are parallel to the cathode ($B_z=0$), we have a maximum value of the

heat flux ($cos^3\ \theta = 1$) while it is negligible where the magnetic induction is perpendicular to the cathode ($B_{xy}=0$ and $cos^3\ \theta = 0$).

III. Heat transfer model

Steady state heat transfer problems are governed by the energy conservation equation

$$\vec{\nabla}(k\vec{\nabla}T)=0 \qquad (7)$$

where k (W m^{-1} K^{-1}) is the thermal conductivity and T (K) the temperature.

The first step in using FEMLAB® heat transfer model is to define the computational domain (figure 4) from the system geometry. The domain is divided into two main parts that are the crucible and the zinc target.

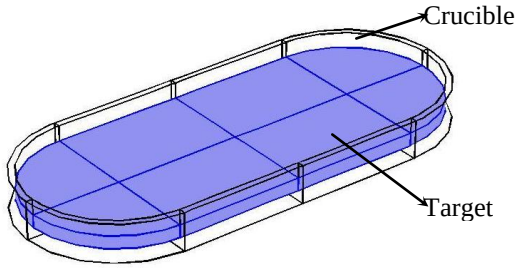

Figure 4. SIP geometry

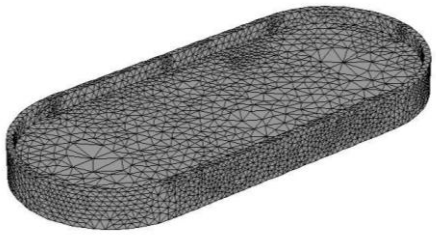

Figure 5. SIP mesh

The mesh (figure 5) of the SIP geometry is composed of 25479 tetrahedral elements and 6360 nodes.

The boundary conditions applied on the different faces of the model are defined on figure 6 :

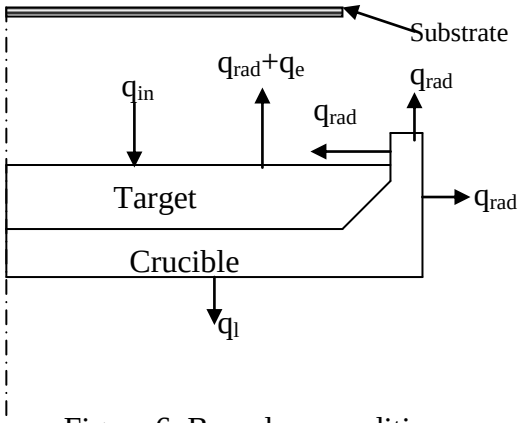

Figure 6. Boundary conditions

1. q_l is the heat loss from the lower crucible surface to the cooling water flow through the insulating powder. It is given by

$$q_l=h(T-T_l) \qquad (8)$$

where h (W m^{-2} K^{-1}) is a global heat loss coefficient and T_l, the temperature of the cooling water.

2. q_{in} is the heat flux applied on the target surface and resulting from the ions bombardment. q_{in} evolves with $\left\{\frac{B_{xy}}{\sqrt{B^2_{xy}+B^2_z}}\right\}^3$ as presented in the magnetic model (II).

3. q_e is the heat flux due to the evaporation of the target material. This boundary condition is defined by

$$q_e = J_e * L_V \tag{9}$$

where J_e (kg $s^{-1}m^{-2}$) is the mass flux of evaporated material and L_v (J kg^{-1}), the latent heat of evaporation.

J_e is defined by the Hertz-Knudsen theory [4] as

$$J_e(\text{kg m}^{-2}\text{s}^{-1}) = 5{,}834\ 10^{-1}\sqrt{\frac{M_t}{T_e}}(p_v - p_{stat}) \tag{10}$$

with M_t (uma), the molecular mass of the target material, T_e (K), the temperature of evaporation, p_v (Torr), the saturation vapor pressure and p_{stat} (Torr), the static pressure.

4. q_{rad} is the radiative heat flux resulting from the temperature differences between the bodies involved in the SIP process. To correctly define the radiative heat transfer condition, a radiation model has been developed and coupled with the FEMLAB® model.

The net radiative heat flux applied on a surface *i* is written

$$q_{irad,net} = \frac{1}{S_i}\sum_j \overline{S_j S_i}\,\sigma\left(T_j^4 - T_i^4\right) \tag{11}$$

Or, with matrix notation,

$$[q_{irad,net}] = \left\{[SS][\sigma T^4] - [\varepsilon]_D[S]_D[\sigma T^4]\right\}[S_i^{-1}] \tag{12}$$

where [SS] is the matrix of total exchange areas and $[\varepsilon]_D$,$[S]_D$, respectively the diagonal matrices of emissivity and element surfaces.

The matrix of total exchange areas [SS] is calculated using the method of Noble[5].

$$[SS] = [R]_D[R]_D[ss]_D \tag{13}$$

$$[R] = \left\{[S]_D - [ss][\rho]_D\right\}^{-1} \tag{14}$$

with [ss], the matrix of direct exchange areas and $[\rho]_D$, the diagonal matrix of reflectivity (ρ=1-ε) of the elements.

To use relation (13) , it is necessary to know the matrix of direct exchange areas. In order to calculate it we use the following approximate equation (figure 7):

$$\overline{s_i s_j} = \frac{\cos\theta_i \cos\theta_j}{\pi R^2}\Delta S_i \Delta S_j \tag{15}$$

where ΔS_j and ΔS_i (m^2) are two elementary surfaces that exchange heat flux by direct radiation, R(m) is the distance between the centers of both elementary surfaces, θ_i and θ_j are the angles between R and the normal to each surface.

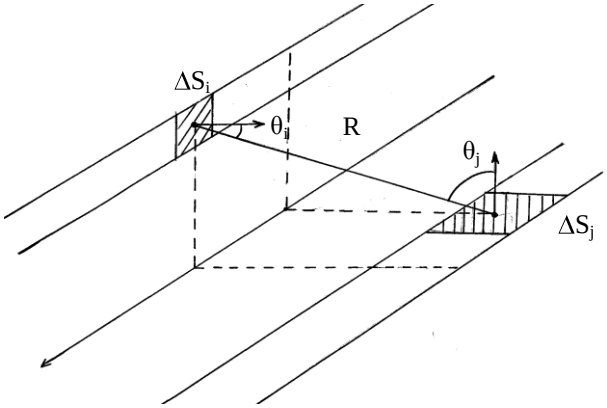

Figure 7. Definition of elementary surfaces

The results of the FEMLAB® model coupled with the radiative model (under MATLAB®) are presented on figure 8.

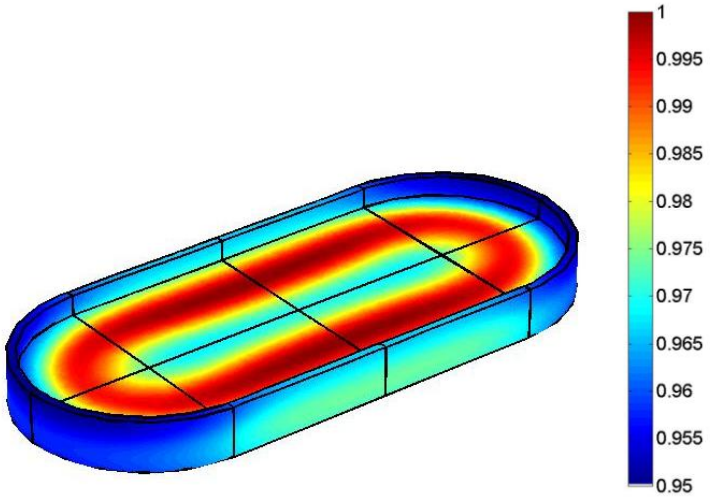

Figure 8. Results of the heat transfer simulation

Figure 8 shows that a track is obtained at the target surface where the temperature (and consequently the erosion) is higher. Those results seem to be in good agreement with reality.

IV. Evaporation model

Knowing the temperature distribution on the target surface, the profile of the coating on the substrate can be determined. To evaluate the coating thickness we use the theory of evaporation [6].

We assume to have (figure 9)

1. a point source (dS_e)
2. no collisions between atoms in the space between the target and the substrate
3. a substrate parallel to the source and located at a distance d

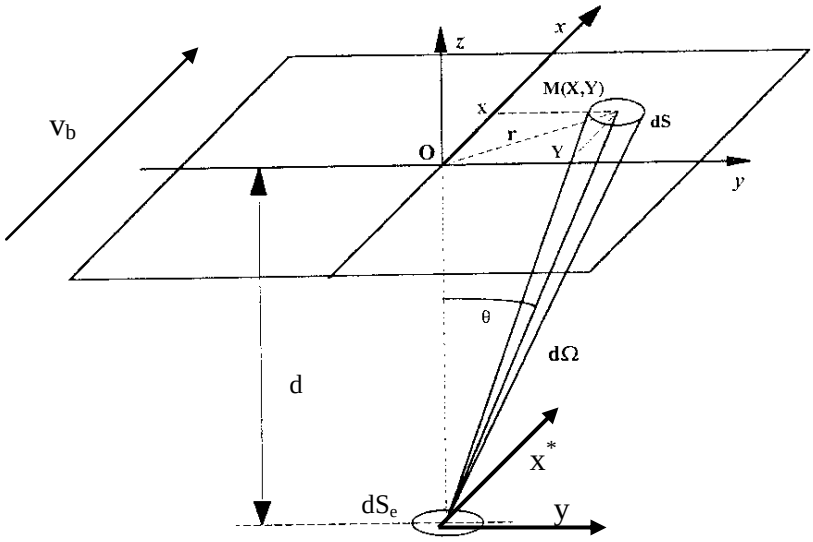

Figure 9. Evaporation model

In this case the mass flow dq_{md} (kg s^{-1}) deposited on the surface element dS around point M is equal to the mass flow evaporated dq_{me} (kg s^{-1}) in the solid angle $d\Omega$.

$$dq_{md} = dq_{me} \tag{16}$$

$$dq_{m_d} = \frac{J_e}{\pi} dS_e \cos\theta \, d\Omega \tag{17}$$

with J_e (kg m^{-2} s^{-1}) given by the Hertz-Knudsen theory (9).

We deduce from figure 9 that

$$d\Omega = \frac{dS \cos\theta}{(r^2+d^2)} \tag{18}$$

$$\cos\theta = \frac{d}{\sqrt{r^2+d^2}} \tag{19}$$

r (m) is the distance between point M and the projection of the point source on the deposition surface and d (m) is the distance between the target and the substrate.

So we can write

$$\frac{dq_{md}}{dS} = dJ_d = \frac{J_e}{\pi} \frac{d^2}{(r^2+d^2)^2} dS_e \tag{20}$$

with dJ_d (kg m^{-2} s^{-1}), the mass flux of deposited material coming from the point source dS_e.
The total mass flux of deposited material J_d, coming from the sources dS_e of an evaporating surface S_e is then given by

$$J_d = \int_{S_e} \frac{J_e}{\pi} \frac{d^2}{(r^2+d^2)^2} dS_e \tag{21}$$

If we consider that the surface dS moves (figure 9) with a velocity v_b (m s^{-1}), the total coating thickness on point $M(X,Y)$ is

$$e_d(X,Y) = \int_0^{\infty} \frac{J_d(x^*,y)}{\rho_e} d\tau \tag{22}$$
$$x^* = v_b \tau$$

where x^*y is a global axis system that is initially identical to the local axis system xy.

Discretizing the displacement of the surface in the x^* direction with $x^*_{i+1} = x^*_i + v_b \Delta t$, we can write

$$e_d(X,Y) = \sum_{i=0}^{n-1} \frac{J_d(x^*_i, Y)}{\rho_e} \Delta t \qquad (23)$$

e_d (m) is the deposit thickness, ρ_e (kg m^{-3}), the density of the evaporated material and Δt, an elementary interval of time.

A program has been developed that simulates the theory of evaporation (21). With the temperature field obtained on the target surface, we are able to determine the thickness of the deposit resulting from the crossing of the band over the top of the SIP system. Figure 10 compares the measured and computed normalised thickness profiles across the steel band.

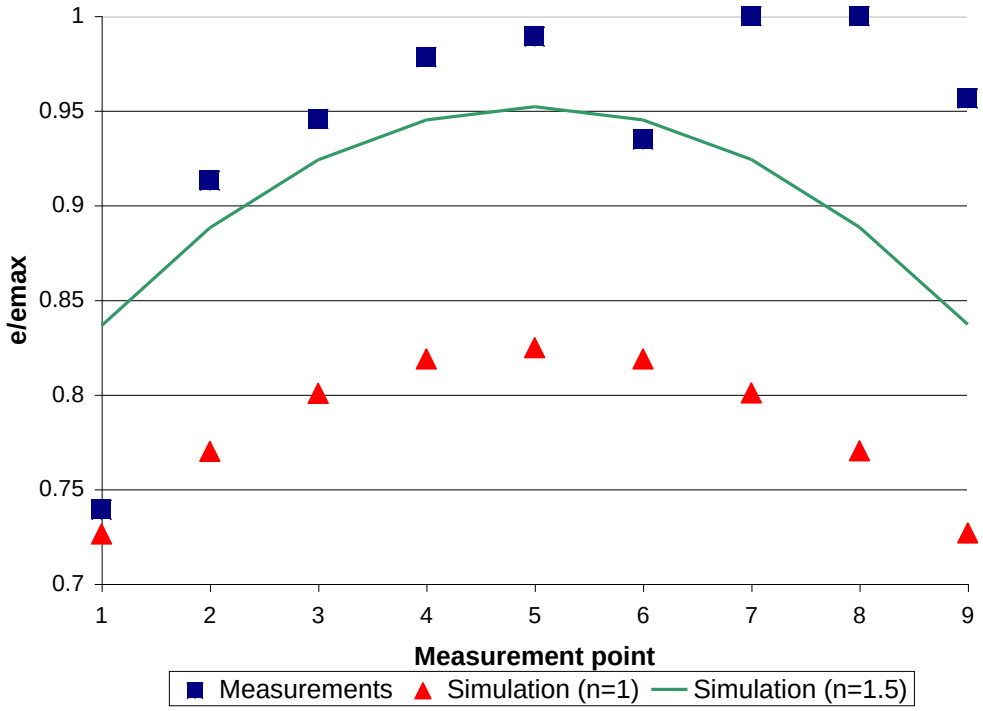

Figure 10. Normalised thickness profile across the band.
(e_{max} , maximum value of measurements)

Figure 11 shows that the qualitative results of this first model of SIP process don't fit precisely the experimental results. Quantitatively, our results underestimate of 17,5 % the maximum value of the thickness.

Nevertheless we note that the measurements don't seem to be accurate because the thickness profile is not symmetrical. That shows that new experiments are required to validate our simulated results.

In addition to those possible measurement errors, we know that several assumptions made to simplify the problem do not agree with the experiments. For example, to introduce the evaporation theory, we have supposed that there were no collisions between atoms during their displacement towards the substrate. This assumption is correct when the mean-free path of the particle is larger than the distance between the target and the substrate. In the current studied setup, it is not the case.

So to take the collisions into account, we should introduce in the theory of evaporation an empirical coefficient *n* such as (21) becomes

$$J_d = \int_{S_e} \frac{(n+1)J_e}{2\pi} \frac{d^{(n+1)}}{(r^2+d^2)^{\frac{(n+3)}{2}}} dS_e \qquad (24)$$

The simulated thickness profile for *n=1,5* is presented on figure 10. We obtain the same profile that for *n=1* but the relative error on the maximum value decreases to 4,8 %.

V. Conclusions and future developments

In this paper we have presented a model of a new vapor deposition technique that we refer to as self-induced ion plating. The model consists of three submodels : a magnetic model, a heat transfer model and an evaporation model. The first one is required in order to simulate the magnetic field generated by the magnetron and to define the profile of the ions bombardement heat flux on the target surface. The heat transfer model defines the heat exchange between all parts of the SIP and, in particular, the radiative heat transfer which is modeled with the method of Noble. The solution of this second model gives the temperature field on the target surface. The third model evaluates the coating thickness profile thanks to the temperature field obtained with the previous model associated with the theory of evaporation. The computational results achieved are compared with measurements. The comparaison shows that our results do not fit the measurements. The reasons lie in some inadequate assumptions but also in the experimental results that don't seem to be very accurate. Hence, in future developpements new experiments are planned to check the validity of the model.

VI. Nomenclature

e	[m] Deposition thickness
d	[m] Distance between evaporation source and deposition point
dS	[m^2] Elementary surface
dΩ	[sr] Elementary solid angle
h	[W m^{-2} K^{-1}] Heat loss coefficient
k	[W m^{-1} K^{-1}] Thermal conductivity
n	Exponent of the evaporation theory
p_v	[Torr] Vapor pressure
p_{stat}	[Torr] Static pressure
q	[W m^{-2}] Heat flux
q_m	[kg s^{-1}] Mass flow
r	[m] Distance between the deposition point and the projection of the point source on the deposition surface
$s_i s_j$	[m^2] Direct exchange area
t	[s] Time
v	[m s^{-1}] Velocity
xy	Local axis system
x* y	Global axis system
B	[T] Magnetic flux density
H	[A m^{-1}] Magnetic field
J	[Kg s^{-1} m^{-2}] Mass flux
L_v	[J kg^{-1}] Latent heat of evaporation
M	[A m^{-1}] Magnetization
M_0	[A m^{-1}] Pre-magnetization

M_t	[u.m.a.] Molecular mass of the target material
R	[m] Distance between the centers of a pair of elementary surfaces
S	[m^2] Surface
S_iS_j	[m^2] Total exchange area
T	[K] Temperature
V_m	[A] Scalar magnetic potential
ε	Emissivity
θ	[radian] Angle
μ_0	[$4\pi\ 10^{-7}$ H m^{-1}] Magnetic permeability of vacuum
μ_r	Magnetic relative permeability
ρ	Reflectivity
ρ_e	[kg m^{-3}] Density of the evaporated material
σ	[$5{,}67\ 10^{-8}$ W m^{-2} K^{-4}] Stephan-Boltzmann's constant

Subscripts

b	Band
d	Deposition
e	Evaporation
l	Loss
in	Input
max	Maximum value
rad	Radiative
xy	Horizontal component
z	Vertical component

VII. References

[1] P. Vanden Brande, A. Weymeersch, *Steel coating by self-induced ion plating, a new high throughput metallization ion plating technique,* J.Vac.Sci.Technol., A18(4), pp. 1555-1560, 2000.

[2] P. Vanden Brande, S. Lucas, and A. Weymeersch, European Patent N° 0780489 (Nov.1996).

[3] Plasma Surface Engineering Corporation, *Technology Note : Magnetron sputtering*, Feb. 2003. Available from Internet : < http// www.msi-pse.com/magnetron_sputtering.htm>.

[4] L. Maissel, R. Glang, *Handbook of thin film technology*, Mc Graw-Hill,1970.

[5] J.M. Rhine, R.J. Tucker, *Modeling of gas-fired furnaces and boilers and other industrial heating processes*, British Gas, Mc Graw-Hill,1991.

[6] D. Chaleix, Ph. D. Thesis, *Etude et modélisation de l'évaporation à grande vitesse par bombardement électronique. Application à la métallisation au défilé de tôles en acier doux par coévaporation*, University of Limoges (France), 1994.

[7] FEMLAB 2.3 User's Guide.